Naval Research Laboratory

Washington, DC 20375-5320

Low-Voltage Infrared Free-Electron Lasers Based on Gyrotron-Powered RF Wigglers

WALLACE M. MANHEIMER
ARNE W. FLIFLET
PHILLIP SPRANGLE

Beam Physics Branch
Plasma Physics Division

November 15, 1996

REPORT DOCUMENTATION PAGE

Public reporting burden for this collection of information is estimated to average 1 hour per response, including the time for reviewing instructions, searching existing data sources, gathering and maintaining the data needed, and completing and reviewing the collection of information. Send comments regarding this burden estimate or any other aspect of this collection of information, including suggestions for reducing this burden, to Washington Headquarters Services, Directorate for Information Operations and Reports, 1215 Jefferson Davis Highway, Suite 1204, Arlington, VA 22202-4302, and to the Office of Management and Budget, Paperwork Reduction Project (0704-0188), Washington, DC 20503.

1. AGENCY USE ONLY (*Leave Blank*)	2. REPORT DATE November 15, 1996	3. REPORT TYPE AND DATES COVERED Interim Report, July 1995 - July 1996	

4. TITLE AND SUBTITLE

Low-Voltage Infrared Free-Electron Lasers Based on Gyrotron-Powered RF Wigglers

5. FUNDING NUMBERS

WU - 5739
TA - 001-09-41

6. AUTHOR(S)

Wallace M. Manheimer, Arne W. Fliflet, and Phillip Sprangle

7. PERFORMING ORGANIZATION NAME(S) AND ADDRESS(ES)

Naval Research Laboratory
Washington, DC 20375-5320

8. PERFORMING ORGANIZATION REPORT NUMBER

NRL/FR/6790--96-9834

9. SPONSORING/MONITORING AGENCY NAME(S) AND ADDRESS(ES)

Office of Naval Research
800 North Quincy Street
Arlington, VA 22217-5660

10. SPONSORING/MONITORING AGENCY REPORT NUMBER

11. SUPPLEMENTARY NOTES

12a. DISTRIBUTION/AVAILABILITY STATEMENT

Approved for public release; distribution unlimited.

12b. DISTRIBUTION CODE

13. ABSTRACT (*Maximum 200 words*)

Designs are presented for infrared free-electron lasers (FELs) with gyrotron-powered electromagnetic wigglers and relatively low-voltage electron beams. The use of an electromagnetic wiggler formed by a quasi-optical gyrotron, where the radiation is coupled into a corrugated waveguide, has the potential for substantial increases of FEL gain compared to an open mirror system. Designs for Proof-of-Principle, low-voltage infrared FEL experiments based on both radio-frequency (RF) linear accelerator and electrostatic technology are presented, together with point designs for portable systems covering the infrared windows in the atmosphere.

14. SUBJECT TERMS

Low-voltage IR FEL
Quasi-optical gyrotron
Electromagnetic wiggler

15. NUMBER OF PAGES

16

16. PRICE CODE

17. SECURITY CLASSIFICATION OF REPORT UNCLASSIFIED	18. SECURITY CLASSIFICATION OF THIS PAGE UNCLASSIFIED	19. SECURITY CLASSIFICATION OF ABSTRACT UNCLASSIFIED	20. LIMITATION OF ABSTRACT UL

NSN 7540-01-280-5500

Low-Voltage Infrared Free-Electron Lasers Based on Gyrotron-Powered RF Wigglers

Wallace M. Manheimer, Arne W. Fliflet, and Phillip Sprangle

Plasma Physics Division
Naval Research Laboratory
Washington, DC 20375

Abstract

Designs are presented for infrared (IR) free electron lasers (FELs) with gyrotron-powered electromagnetic wigglers and relatively low voltage electron beams. The use of an electromagnetic wiggler formed by a quasi-optical gyrotron, where the radiation is coupled into a corrugated waveguide, has the potential for substantial increases of FEL gain compared to an open mirror system. Designs for Proof-of-Principle low voltage infrared FEL experiments based on both radio-frequency (RF) linear accelerator and electrostatic accelerator technology are presented together with point designs for portable systems covering the infrared windows in the atmosphere.

CONTENTS

LOW-VOLTAGE INFRARED FREE-ELECTRON LASERS BASED ON GYROTRON-POWERED RF WIGGLERS

1. INTRODUCTION

There is currently considerable interest in compact, tunable infrared (IR) radiation sources operating in the vibrational IR spectrum (3–30 μm) [1]. Free-electron lasers (FELs) capable of operating in this regime have been developed at a small number of fixed sites around the world. However, there is a need for portable systems capable of operating in the 3–5 and 8–13 μm atmospheric windows for remote sensing applications. Wider use of FELs is inhibited by system size, cost, and the shielding requirements associated with the production of high-current, 15–45 MeV electron beams that are currently needed to lase in the infrared. The required electron beam energy, $E = \gamma mc^2$, where m is the electron rest mass, c is the speed of light, and γ is the relativistic factor, is related to the output wavelength (λ_s) and the wiggler period (λ_0) according to

$$\gamma = \sqrt{\frac{\lambda_0 \left(1 + a_{\mathrm{w}}^2\right)}{2\lambda_s}} \tag{1}$$

for a conventional magnetostatic wiggler, where a_{w} is the root-mean-square (rms) wiggler parameter. The factor $\left(1 + a_{\mathrm{w}}^2\right)$ accounts for the fact that the electron beam's forward velocity is reduced by the quiver motion in the wiggler. In spite of considerable effort, the period of magnetostatic wigglers has so far been constrained to a minimum wavelength of ≈ 1 cm, with 3 cm being more typical. The concept of an electromagnetic wiggler in which the magnetostatic wiggler system of fixed transverse magnets is replaced by an intense counterstreaming microwave or optical radiation beam has been of interest from the early work on FELs as a means of reducing the required electron-beam energy [2]–[9]. This now becomes

$$\gamma = \sqrt{\frac{\lambda_0 \left(1 + a_{\mathrm{w}}^2\right)}{2 \left(1 + k_{\|}/k\right) \lambda_s}}, \tag{2}$$

where the term $k_{\|}/k$ ($k = 2\pi/\lambda_0$ is the wavenumber of the wiggler radiation, and $k_{\|}$ is its axial component) in the factor $\left(1 + k_{\|}/k\right)$ accounts for the fact that the wiggler radiation may be confined in a waveguide. Although there has been little experimental progress to date due to the lack of high-power wiggler-radiation sources, the recent development of high-power millimeter-wave gyrotrons has led to a re-evaluation of the feasibility of electromagnetic wigglers [10]–[12]. We have published earlier studies of the possibility of IR FELs based on low

energy beams (3–5 MeV) using a gyrotron-powered millimeter-wave wiggler [13]–[16]. The wiggler radiation forms a standing mode in a high-Q resonator through which the electron beam propagates and interacts with the counterstreaming wave of the standing mode. Both the waveguide cavity gyrotron and the quasi-optical gyrotron (QOG) configurations were considered. The QOG is based on an open-mirror resonator and is particularly suitable for use as a wiggler because of its ability to operate at short wavelength with high efficiency, high circulating power, and long pulse lengths. In the QOG-wiggler design analyzed previously, the wiggler radio-frequency (RF) fields were provided by a Gaussian mode in an open-mirror resonator. Limits in the achievable wiggler RF power density in an open resonator led to the prediction of rather modest single-pass FEL gains of a few percent. This report presents a new wiggler design in which the RF power generated by the QOG is coupled into a corrugated waveguide and compressed. This has the possibility of substantially increasing FEL gain over previously published design concepts.

1.1. Electron Accelerators

In previous work, the basic requirements on the electron beam for application to millimeter-wavelength electromagnetic wigglers have been presented. Two accelerator technologies have been identified as being capable of meeting these requirements: the electrostatic linac (ES-linac) and the RF-linac with a laser photocathode. Both are capable of generating the low emittance beams necessary for high FEL gain and efficiency where we define the emittance as $1/\pi$ times the area in $r - r'$ space ($r' = dr/dz$) occupied by the beam electrons (in cylindrical coordinates). It is common practice to express the emittance requirement in terms of the normalized emittance $\varepsilon_n = \gamma\beta\varepsilon$, where $\beta = v_z/c$ and v_z = axial velocity. Each configuration has advantages for FEL operation, and either is reasonably compact. For example, the 3 MeV ES-accelerator shown in Fig. 1 is approximately 16 ft in length and 4 ft in diameter, compact enough to fit in a small facility or be transported on a truck, train, ship, or aircraft. The ≈ 5000 lb weight could be reduced to ≈ 2000 lb by using titanium instead of steel for the tank material. Since the beam is recirculated with near complete charge recovery, minimal radiation shielding is necessary. Another example is the 6 MeV ES-linac FEL at the University of California at Santa Barbara (UCSB)[17]. This facility produces a high-quality electron beam with a normalized emittance of 10-mm mrad and could drive a QOG–wiggler FEL with little modification. Such a wiggler would allow this facility, which currently operates in the far-IR, to lase in the vibrational IR—a major advance.

The size of RF linacs is even more compact and does not increase very rapidly with beam energy. A particularly compact form of RF accelerator, called the "RF gun" (RFG), has recently been applied to FELs. Lewellen et al.[18] have developed a far-IR FEL (80–300 μm) at Stanford based on an 8-cm long, $1\frac{1}{2}$ cell, S-band RFG with a thermionic cathode. The RFG produces an electron beam with up to 4.5 MeV kinetic energy, a 6 A micropulse current, a normalized emittance of 7 mm-mrad, a micropulse length of 10 ps, and an energy spread of 1%. A similar RFG is currently being set up at the Naval Research Laboratory (NRL). An RFG with a laser photocathode has been developed for an FEL by Northrup-Grumman [19]. The Northrup-Grumman FEL, designed to operate at wavelengths from 10 to 20 μm, uses a 20-cm long, $3\frac{1}{2}$ cell, S-band RFG that produces beam energies up to 9 MeV with $\sim$ 1 nC of

Figure 1: The 3 MeV tandem electrostatic accelerator built by NEC

charge per micropulse and a micropulse length of 5 ps. The laser photocathode operates at 142.8 MHz, the beam emittance is estimated to be 2.7–10 mm-mrad, and the energy spread can be as low as 0.1% depending on the pulse length. A schematic of a $2\frac{1}{2}$-cell, S-band RFG with a laser photocathode capable of producing a 6 MeV, high-brightness electron beam, is shown in Fig. 2. The beam from such an RFG, coupled to a QOG-powered wiggler, gives rise to the possibility of a RFG-powered IR FEL with a smaller footprint and reduced shielding compared to existing systems.

2.   QOG-CORRUGATED WAVEGUIDE WIGGLER

As discussed above, a difficulty of the open-mirror resonator configuration for an electromagnetic wiggler is that the wiggler radiation diffracts freely as it propagates. The smaller the radiation beam waist (desirable for high-power density), the shorter the Rayleigh length, which defines the effective length of the wiggler. One way of overcoming this limitation is to confine the wiggler radiation in a waveguide. This approach has been examined by Danly et al. [10] and Fliflet et al. [16] in the context of waveguide gyrotrons. Since there are definite advantages to a QOG-based configuration in other respects, it is of interest to see if a means of overcoming this limitation can be found. The use of corrugated waveguide offers a solution [20].

A smooth-walled circular waveguide wiggler could employ the TE_{11} or higher order TE_{1n} mode since such modes are peaked on axis. However, these modes have a number of disadvantages, including: (1) significant wall losses at high power levels, (2) susceptibility to mode conversion at waveguide irregularities, and (3) low conversion efficiency into free-space modes. As pointed out by Efthimion [20], the use of the HE_{11} mode in a corrugated waveguide
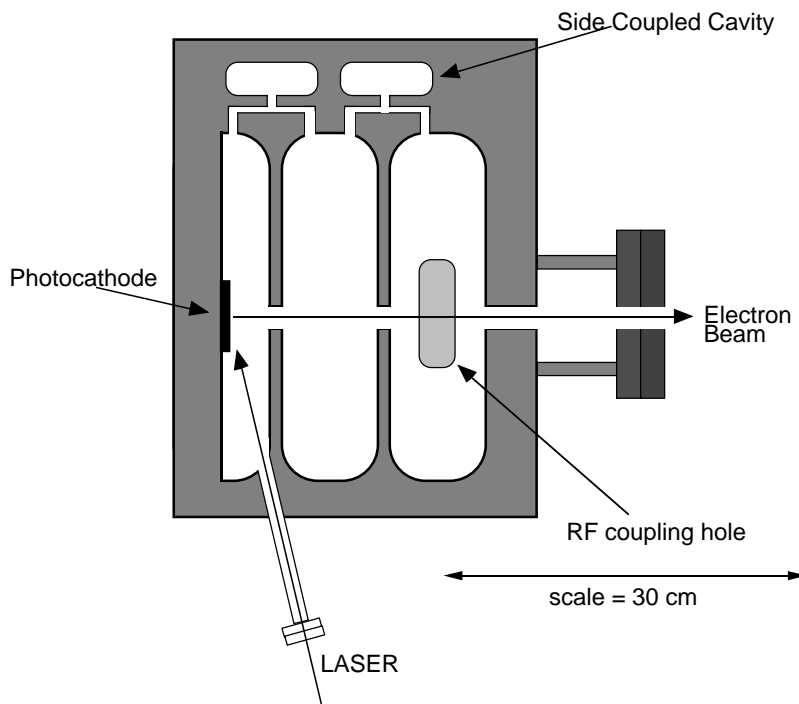
Figure 2: The $2\frac{1}{2}$-cell, S-band RFG accelerator with laser photocathode

represents an attractive alternative. Corrugated waveguides have been successfully applied to the transfer of high-power mm waves from gyrotrons to tokamaks [21]. If the depth and period of the corrugation are $\approx \lambda_0/4$, the HE_{11} mode has only an H_z component of the magnetic field tangential to the wall surface, i.e., the azimuthal component $H_\phi \approx 0$. Moreover, the H_z component is small, less than that of the TE_{01} mode in the same size waveguide [22], and the ohmic loss is correspondingly low. Since the HE_{11} mode is well separated from competing modes, propagation is insensitive to waveguide irregularities. Finally, the HE_{11} mode at an open-ended corrugated waveguide couples efficiently to the fundamental free-space Gaussian mode.

In a corrugated waveguide, the axial components of the electric and magnetic fields are generally both required to satisfy the boundary conditions. Low-loss propagation of the HE_{11} mode occurs when the waveguide is designed such that the ratio of these components satisfies

$$\left| \frac{E_z}{H_z} \right| = \sqrt{\frac{\mu_0}{\epsilon_0}}, \tag{3}$$

(except in the region of the corrugations), where ϵ_0 and μ_0 are the permittivity and permeability of free space, respectively. In corrugated waveguide terminology, this is called the balanced hybrid condition. In this case, the RF fields of HE_{11} mode are, to a good approximation, linearly polarized with the transverse form [22]

$$E_x = E_0 J_0 \left(k_t r \right), \tag{4}$$

and

$$H_y = \frac{E_0}{Z_0} \mathrm{J}_0 \left(k_t r \right), \tag{5}$$

where k_t is the transverse component of the wiggler waveumber, J_0 is a regular Bessel function, r is the radial coordinate, and $Z_0 = 377\ \Omega$. Meter-kilogram-second (MKS) units are used throughout. Since there is no axial current or tangential electric field at the waveguide wall, $r = a$ (a is also assumed to be much larger than the corrugation depth), the condition on the transverse wave number k_t is $k_t a = 2.4$, the first zero of the Bessel function. The dispersion relation is given by

$$\omega_0^2 = (k_{||}^2 + k_t^2)c^2, \tag{6}$$

where ω_0 is the angular frequency of the wiggler RF fields. The actual calculation of the fields in the corrugated waveguide is quite complicated; however, Eqs.(4-6) are reasonable approximations for the balanced hybrid condition. Near the axis, the electric field of the counterpropagating wave is given by

$$E_x = \frac{mc\omega_0}{\sqrt{2}e} a_\mathrm{w} e^{i\left(k_{||}z + \omega_0 t\right)} + \mathrm{c.c.}, \tag{7}$$

where e is the electron charge, and the rms on-axis wiggler parameter for the the HE_{11} mode is given by

$$a_\mathrm{w} = \frac{1}{2\sqrt{2}\pi \mathrm{J}_1(2.4)} \frac{\lambda_0}{a} \sqrt{\frac{P_\mathrm{w}}{P_0}}, \tag{8}$$

where P_w is the wiggler circulating power and $P_0 = 1.09 \times 10^9$ W.

The HE_{11} corrugated waveguide mode couples extremely well to the free-space Gaussian mode [23]: the coupling efficiency is 98%, if the Gaussian mode beam waist is given by $w_0 = 0.6435a$. Thus if the corrugated waveguide is inserted in the quasi-optical resonator with appropriate matching, the round-trip losses for the wiggler radiation will be about 4%. As discussed above, the HE_{11} mode has low ohmic losses. These losses are negligible in the configurations we present. A schematic of the proposed electromagnetic wiggler FEL configuration is shown in Fig. 3.

As shown previously [16], the peak warm-beam gain is given by

$$\begin{aligned}
G \;=\; & 2\pi^3 f \frac{I}{I_A} \frac{\lambda_s^{3/2}\lambda_0^{1/2}}{\sigma_s} a_\mathrm{w}^2 N^3 (0.27) \\
& \left[1 + \left(2N\frac{\Delta\gamma}{\gamma}\right)^2 + \left(\frac{2N\varepsilon_n^2}{r_b^2}\right)^2 + \left(\frac{2NI}{I_A\gamma}\right)^2 + \left(Na_\mathrm{w}^2 k_t^2 r_b^2\right)^2\right]^{-1},
\end{aligned} \tag{9}$$

where I is the beam current, $I_A = 17$ kA, $N = 2L/\lambda_0$ is the number of wiggler periods encountered by the electron beam during the interaction, L is the interaction length, and σ_s is the effective FEL mode area given by $\sigma_s = \pi w_s^2/2$, where w_s is the FEL Gaussian beam waist. The Rayleigh length, $z_s = \pi w_s^2/\lambda_s$, of the FEL beam must be at least $L/2$. The filling factor $f = 1$, if the electron beam cross section (σ_b) is $\le \sigma_s$, otherwise $f = \sigma_s/\sigma_b$. The conditions needed to match the electron beam cross-section to the FEL beam (filling factor
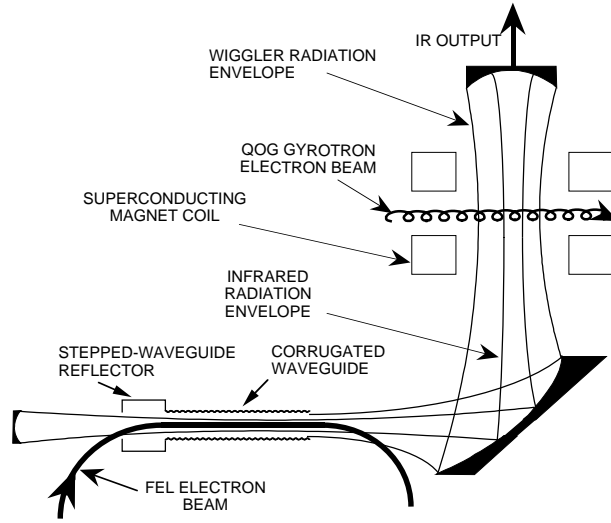
Figure 3: The EMFEL with hybrid QOG–corrugated waveguide wiggler

of one) can be illustrated using the beam-envelope equation (assuming a highly relativistic beam with an applied magnetic field but generated from a shielded cathode):

$$\frac{\partial^2 r_b}{\partial z^2} + \frac{\Omega^2}{4c^2\gamma^2 r_b} - \frac{2I}{I_A\gamma^3 r_b} - \frac{\varepsilon_n^2}{\gamma^2 r_b^3} = 0, \tag{10}$$

where the fact that $\beta \approx 1$ for a highly relativistic beam has been used, and Ω is the nonrelativistic cyclotron frequency. A matched beam with a constant radius (first term on left side of Eq.(10) = 0) can be obtained by injecting the beam into a solenoidal magnetic field

$$B_0 = \frac{mc}{|e|}\sqrt{\frac{8I}{I_A\gamma r_b^2} + \frac{4\varepsilon_n^2}{r_b^4}}, \tag{11}$$

with suitable focussing elements. Alternatively, for an emittance-dominated beam and no applied magnetic field, Eq.(10) has the solution [24]

$$r_b(z) = r_b(0)\sqrt{1 + \frac{\varepsilon^2 z^2}{r_b^4(0)}}. \tag{12}$$

Thus in this regime, the electron-beam profile can be matched to the profile of a Gaussian FEL mode, if the emittance satisfies $\varepsilon < \lambda_s/\pi$ [24]. The terms in the denominator of Eq.(9) account for resonance detuning effects associated with energy spread ($\Delta\gamma$), normalized emittance, space charge, and transverse wiggler gradients. Unlike conventional magnetostatic wigglers, transverse wiggler gradients are negligible. Equation(9) corrects an error in previous publications [13]–[16] in which the space-charge detuning effect was overestimated by a factor of γ.

As shown by Antonsen and Levush [25] for a magnetostatic wiggler configuration, the nonlinear operation of a low-gain FEL oscillator with a cold beam can be characterized by two universal parameters—the normalized detuning parameter $\Delta\mathcal{P}_{\text{inj}}$ and the normalized average beat-wave amplitude $\bar{\mathcal{A}}$. The results of this theory are given by the FEL oscillator's "universal operating map," which expresses the normalized electronic efficiency $\Delta\mathcal{P}$ in terms of these parameters. Extension of this theory to the electromagnetic wiggler case has been discussed previously [15, 16], and the principal results are as follows. The electronic efficiency is given by

$$\eta = \frac{\Delta\mathcal{P}}{4\pi N},\tag{13}$$

the rms circulating power in the FEL resonator at saturation is given by

$$P_s = \frac{P_0\gamma^2\bar{\mathcal{A}}^2}{4\pi^4 N^3 a_{\text{w}}^2},\tag{14}$$

and the per-pass output coupling required for steady-state operation at given values of $\bar{\mathcal{A}}$ and $\Delta\mathcal{P}$ is given by

$$T = \frac{14.8\Delta\mathcal{P}G}{\bar{\mathcal{A}}^2}.\tag{15}$$

Reference to the universal operating map shows that the optimum values of $\Delta\mathcal{P}$ and $\bar{\mathcal{A}}$ for a cold beam are 5.5 and 18, respectively [25]. These expressions are valid provided that thermal effects are sufficiently small and that the gain is not greatly reduced from the cold beam value.

The laser lethargy effect, which results from the fact that during the interaction the radiation beam slips ahead of the electron by $N\lambda_s$, must be considered for an IR FEL based on an RFG. To avoid loss in interaction efficiency, this distance should be much less than the radiation pulse length l_p, i.e., the ratio $s = N\lambda_s/l_p$ should satisfy $s \ll 1$. This places a constraint on the maximum number of wiggler periods and affects the coherence, since the linewidth due to this effect is $\delta\omega/\omega \sim \lambda_s/l_p$ [26].

3. ELECTROMAGENETIC WIGGLER FEL DESIGNS

In this section, two RFG-based FEL point designs and four ES-linac-based FEL point designs are presented. A Proof-of-Principle (PoP) design is proposed for each accelerator type along with designs requiring further development. The prescription used in obtaining the design configurations has been discussed previously [13]–[16]. In each case, the wiggler is based on a QOG with with sufficient intracavity circulating power to provide per-pass FEL gain of at least 10% and sufficient output power to offset wiggler resonator losses of 8%. The QOG parameters are given in Table 1. In the ES-linac-based configurations (Configurations 3–6), the QOG circulating power is 20 MW. This choice is motivated by an NRL experimental QOG that has generated over 20 MW of intracavity power and has an output power of 0.6 MW (corresponding to 3% output coupling) at 120 GHz for a 10 μs pulse length [27]. The required output power scaling to 8% can be achieved by doubling the QOG efficiency obtained in this experiment using mode-priming techniques [28] and by operating the QOG at higher current. In the RFG-based configurations (Configurations 1

and 2), the circulating power is 42 MW, which can be achieved by using a high-power magnetron-injection-gun (MIG)-type electron gun developed jointly by NRL and Varian (now Communications Power Industries (CPI)), model number VUW-8101 [29].

Table 1: Parameters of QOG Wigglers

Configuration	1	2	3	4	5	6
QOG–Wiggler Wavelength (mm)	2.7	2.7	2.5	2.1	1.5	0.65
Electron Gun Voltage (kV)	150	150	100	100	100	100
Electron Gun Current (A)	122	122	84	84	84	84
Cyclotron Harmonic	1	1	1	1	2	2
Magnetic Field (kG)	51	51	51	60	42	97
Peak Circulating Power (MW)	42	42	20	20	20	20
Peak Output Power (MW)	3.4	3.4	1.6	1.6	1.6	1.6

As shown in Fig. 3, the quasi-optical resonator has two legs: a vertical leg, which contains the QOG interaction, and a horizontal leg, which contains the FEL interaction. The wiggler radiation in the horizontal leg is focussed into a corrugated waveguide that confines it during the FEL interaction. Only the counterpropagating component of the standing-wave resonator mode participates in the FEL interaction [11]. The FEL output radiation is contained in an optical resonator. Optimum gain is obtained by matching the FEL electron-beam cross section to the beam waist of the FEL resonator mode as described. The corrugated waveguide confining the wiggler radiation beam must be large enough that the FEL radiation beam is unaffected by its presence. A solenoidal magnetic field may be used to confine the electron beam in the wiggler; however, since the beams in these designs all satisfy $\varepsilon < \lambda_s/\pi$, it should be possible to match the electron beam to the FEL mode without a solenoidal field. The FEL radiation is taken out at the left. Here the waveguide terminates in a stepped waveguide reflector, which does not impede the electron or IR beams but provides nearly complete reflection ($\sim 99\%$) of the wiggler radiation beam [30]. The wiggler round-trip losses are at least 4% going into and out of the corrugated waveguide. There is another percent or so loss from depolarization at the corner elliptical mirror and perhaps another one or two percent from various other losses. We assume that the total wiggler radiation loss per pass is 8%. However, it is possible to define less efficient FELs with 10% or even 12% losses in the wiggler resonator.

3.1.   RFG Point Designs

Parameters for the two RFG point designs are summarized in Table 2. Configuration 1 represents a Proof-of-Principle experiment that could be carried out using available capital equipment. The nominal output wavelength is 8 μm, however, the wavelength can be varied over a wide range by varying the FEL beam energy. This results in higher power but lower gain at shorter wavelengths, and the converse is true. Configuration 1 is based on a RFG operating at 4.3 MeV with a laser photocathode. The photocathode provides the high

micropulse current, relatively low energy spread, and low emittance needed to achieve high gain with an electromagnetic wiggler. The design is based on a 2.7-mm wavelength, 30-period wiggler. The peak micropulse current is 200 A, and the full-width half-maximum (FWHM) energy spread is 1%. The micropulse length is 5 ps, or 1.5 mm, which is greater than the lethargy slip of 0.2 mm during the wiggler transit. The resulting warm beam gain is 11% and a peak micropulse beam power is 13.7 MW. To achieve saturation with a macropulse of a few microseconds duration, the laser cathode repetition rate should be at least 100 MHz. Since the beam (and, of course, the FEL radiation) is only present for a duty cycle of 5×10^{-4} during the macropulse, the average IR beam power at saturation is about 7 kW. The klystron power required during the macropulse is about 10 MW. Assuming the RFG klystron and QOG are 40% and 20% efficient, respectively, the overall FEL efficiency is $\sim 10^{-4}$, not including the power required for the photocathode laser. Configuration 2 operates at 4 μm with a beam energy of 6.3 MeV and requires somewhat lower beam emittance and energy spread than Configuration 1. The lower current (100 A vs 200 A) is compensated by an increased interaction length (50 vs 30 wiggler periods) to achieve similar gain. Compared to a conventional RF-linac-powered FEL operating in the mid-IR, these designs offer significant reductions in the total power and shielding required.

Table 2: Parameters of IR FELs Based on RFG Accelerators

Configuration	1	2
FEL Wavelength (μm)	8	4
Electron Beam Energy (MeV)	4.32	6.31
Electron Beam Current (A)	200	100
Normalized Emittance (mm mrad)	15	10
Relative Energy Spread (%)	1.0	0.5
Electron Beam Diameter (mm)	0.32	0.32
FEL Mode Beam Waist Diameter (mm)	0.46	0.46
Wiggler Waveguide Diameter (mm)	4.74	4.74
N (wiggler periods)	30	50
Interaction Length (cm)	4.05	6.75
Cold Beam Efficiency (%)	1.5	0.93
Lethargy Slip (mm)	0.21	0.25
a_{w} (rms)	0.049	0.049
Solenoidal Focussing Field (kG)	22.5	17.3
Cold Beam Gain per Pass (%)	18.4	15.1
Warm Beam Gain per Pass (%)	11.0	10.7
Output Coupling per Pass (%)	5.1	4.2
Peak Output Power (MW)	13.7	5.8

3.2.   ES-Linac Point Designs

The ES-linac configurations (Configurations 3–6) have 640 period wigglers. Configuration 3 is based on the beam parameters of the 6 MeV, 2 A UCSB ES-linac [17], and the wiggler wavelength is 2.5 mm. The QOG is assumed to operate at the fundamental cyclotron harmonic with a 51 kG magnetic field as in the NRL experiment. Configuration 3 generates about 8.7 kW at 4 μm, and the warm beam gain is $\sim$ 11%. In this system, most of the prime power is used to drive the QOG, since the ES-linac is relatively efficient as a result of beam energy and current recirculation. Considering that QOG output power is 1.6 MW and the QOG is about 19% efficient (which can be increased to 30% with a depressed collector), the overall FEL efficiency is about 0.1% (or 0.15%). Since the ES-linac at 2 A can potentially be operated dc, the maximum average power is determined by the duty factor of the QOG; for example, a duty factor of 5% produces an average power of 435 W.

Table 3: Parameters of IR FELs Based on ES Linacs

Configuration	3	4	5	6
FEL Wavelength (μm)	4	11	8	3.5
Electron Beam Energy (MeV)	5.97	3.08	3.05	3.03
Electron Beam Current (A)	2	2	2	2
Normalized Emittance (mm mrad)	10	10	7.5	5
Relative Energy Spread (%)	0.02	0.02	0.02	0.02
Electron Beam Diameter (mm)	1.0	1.54	1.1	0.48
FEL Mode Beam Waist Diameter (mm)	1.42	2.16	1.56	0.68
Wiggler Waveguide Diameter (mm)	6.12	6.62	4.72	2.04
N (wiggler periods)	640	640	640	640
Interaction Length (cm)	80	67.2	48	20.8
Cold Beam Efficiency (%)	0.073	0.076	0.076	0.076
a_{w} (rms)	0.024	0.019	0.019	0.019
Solenoidal Focussing Field (kG)	1.5	1.0	1.4	3.3
Cold Beam Gain per Pass (%)	15.0	16.4	16.6	16.7
Warm Beam Gain per Pass (%)	11.4	15	15	12.3
Output Coupling per Pass (%)	4.2	4.6	4.6	4.6
Peak Output Power (kW)	8.67	4.68	4.64	4.61

Configurations 4–6 represent potentially portable FELs based on the 3 MeV ES-linac shown in Fig. 1. As mentioned, a 3 MeV ES-linac is compact enough to fit on a truck or large aircraft. Assuming near total charge recirculation, the FEL electron beam generates little X-ray radiation, possibly requiring only localized shielding to achieve background exposure levels. In Configuration 4, the wiggler wavelength is 2.1 mm, which can be provided by a current state-of-the-art QOG with a 60 kG magnetic field operating at the fundamental cyclotron harmonic. Output wavelengths down to 11 μm provide coverage of the long wavelength region of the 8–13 μm atmospheric window. The peak output power is 5 kW. In Configuration 5, the output wavelength has been reduced to 8 μm by reducing the QOG

wiggler wavelength to 1.5 mm; this is accomplished by operating at the second cyclotron harmonic with a 42 kG magnetic field. Stable second-harmonic operation requires suppression of the fundamental cyclotron harmonic interaction. This may be achieved by replacing the upper mirror of the vertical resonator leg with a diffraction grating placed in the Littrow position [31]. Alternatively, the QOG could be operated at the fundamental cyclotron harmonic by increasing the magnetic field to 84 kG, achievable by using a niobium-tin superconducting magnet. The beam emittance has been reduced to 7.5 mm-mrad from 10 mm-mrad to avoid loss of warm beam gain. Finally, Configuration 6 achieves an output wavelength of 3.5 μm by using a 0.65-mm QOG wiggler. This requires a 97 kG superconducting magnet, approaching the limit of the current superconducting magnet technology and operation at the second harmonic. The assumed beam emittance is 5 mm-mrad.

4.   CONCLUSIONS

The recent development of compact accelerators with high-quality electron beams and of high-power gyrotrons operating in the millimeter and submillimeter wavelength regime has opened the possibility of FELs with electromagnetic wigglers. The designs presented in this report show that the technology needed to demonstrate lasing in the vibrational IR either exists or is close at hand. Suitable electron-beam accelerators can be found in the laboratories of a number of universities, companies, and government organizations. The wiggler designs presented here are based on the QOG developed at NRL. The assumed parameters for Configurations 1 and 2 represent the use of a higher voltage QOG and a state-of-the-art RFG. Configuration 3 represents an upgraded but basically existing gyrotron used in the UCSB facility. Configurations 4–6 represent portable (low-weight and shielding) FELs operating in various regions of the atmospheric propagation windows. Depending on the gyrotron parameters, operation will be in either the long wavelength half of the 8–13 μm window, the entire 8–13 μm window, or both the 3–5 μm and 8–13 μm windows.

5.   ACKNOWLEDGMENTS

REFERENCES

1. D. D. Dlott and M. D. Fayer, "Applications of Infrared Free-Electron Lasers: Basic Research on the Dynamics of Molecular Systems," *IEEE J. Quant. Elect.* **27**, 2697 (1991).

2. R. H. Pantell, G. Soncini, and H. E. Puthoff, "Stimulated Photon–Electron Scattering," *IEEE J. Quant. Electron.* **QE-4**, 905 (1968).

3. P. Sprangle and T. Smith, "Theory of Free-Electron Lasers," *Phys. Rev. A***21**, 293 (1980).

4. L. R. Elias, "High-Power, CW, Efficient Tunable (UV through IR) Free-Electron Laser using Low-Energy Electron Beams," *Phys. Rev.Lett.* **42**, 977 (1979).

5. J.A. Pasour, P. Sprangle, C.M. Tang, and C.A. Kapetanakos, "High-Power, Two-Stage FEL Oscillator Operating in the Trapped Particle Mode," *Nucl. Instrm. Methods Phys. Res.* **A237**, 154 (1985).

6. V. L. Granatstein, Y. Carmel, and A. Gover,"Demonstration of a Free Electron Laser with an Electromagnetic Wiggler," in *Free-Electron Generators of Coherent Radiation* SPIE Proceedings **453**, 344 (1983).

7. A. Gover, C.M. Tang, and P. Sprangle, "Feasibility of D.C. to Visible High Power Conversion Employing a Stimulated Compton Free-Electron Laser with a Guided Wave CO_2 Laser Pump Wave and an Axial Electric Field," *J. Appl. Phys.* **53**, 124 (1982).

8. J. Gea-Banacloche, G. T. Moore, R. R. Schlicher, M. O. Scully, and H. Walther, "Soft X-ray Free-Electron Laser with a Laser Undulator," *IEEE J. Quant. Electron.* **QE-23**, 1558 (1987).

9. J. Gea-Banacloche, G. T. Moore, R. R. Schlicher, M. O. Scully, and H. Walther, "Proposal for a Compact FEL with Electromagnetic-Wave Undulator," *Nucl. Instrm. Methods Phys. Res.* **272**, 199 (1988).

10. B. G. Danly, G. Bekefi, R. C. Davidson, R. J. Temkin, T. M. Tran, and J. S. Wurtele, "Principles of Gyrotron Powered Electromagnetic Wigglers for Free-Electron Lasers," *IEEE J. Quant. Electron.* **QE-23**, 103 (1987).

11. T. M. Tran, B. G. Danly, and J. S. Wurtele, "Free-Electron Lasers with Electromagnetic Standing Wave Wigglers," *IEEE J. Quant. Electron.* **QE-23**, 1578 (1987).

12. T.S. Chu, B.G. Danly and R. Temkin, "A Gyrotron-Powered Standing-Wave Electromagnetic Wiggler Experiment," *Nucl. Instrm. Methods Phys. Res.* **285**, 246 (1989).

13. A.W. Fliflet and W.M. Manheimer, "Compact Infrared Long-Pulse Free-Electron Laser," NRL Formal Report 9504, December 1992.

14. A.W. Fliflet, R.P. Fischer, and W.M. Manheimer, "New Results and Applications for the Quasioptical Gyrotron," *Phys. Fluids B* **5**, 2682 (1993).

15. W.M. Manheimer and A.W. Fliflet, "Long-Pulse, Low-Voltage Infrared Free-Electron Laser," *IEEE Trans. Quant. Electron.* **30**, 185 (1994).

16. A.W. Fliflet, R.P. Fischer, and W.M. Manheimer, "Designs for an Infrared Free-Electron Laser Based on Gyrotron-Powered Electromagnetic Wigglers," *IEEE Trans. Plasma Sc.* **22**, 638 (1994).

17. G. Ramian, "Properties of the New UCSB Free-Electron Lasers," *Short-Wavelength Radiation Sources*, Phillip Sprangle, ed., Proc. SPIE **1552**, 69 (1991).

18. J. W. Lewellen, J. F. Schmerge, Y. C. Huang, J. Feinstein, and R. H. Pantell, "Preliminary Emission Characteristic Measurements for a \$300K FIR FEL," *Nucl. Instrm. Methods Phys. Res.* **A358**, 24 (1995).

19. I. S. Lehrman, J. Krishnaswamy, and R. A. Hartley, "The Northrup Grumman Compact Infrared FEL (CIRFEL)," *Proceedings of the 1995 Particle Accelerator Conference*, IEEE Catalog Number 95CH35843, 260 (1996).

20. P. Efthimion, private communication, November 1992.

21. J. L. Doane, "Mode Converters for Generating the HE 11 (Gaussian-Like) Mode from TE 01 in a Circular Waveguide," *Int. J. Electron.* **53**, 573 (1982).

22. P. Clarricoats and A. Oliver, *Corrugated Horns for Microwave Antennas* (Peter Peregrinus Ltd, Exeter, England, 1984).

23. J. C. G. Lesurf., *Millimetre-wave Optics, Devices and Systems* (IOP Publishing Ltd., Bristol, England, 1990), Chap. 4.

24. C. W. Roberson and P. Sprangle, "Review of Free Electron lasers," *Phys. Fluids* **B1**, 3 (1989).

25. T. M. Antonsen and B. Levush, "Mode Competition and Suppression in Free Electron Laser Oscillators," Phys. Fluids **1**, 1097 (1989).

26. T. C. Marshall, *Free-Electron Lasers* (MacMillan, New York, 1985), p. 60.

27. T. A. Hargreaves, A. W. Fliflet, R. P. Fischer, M. L. Barsanti, W. M. Manheimer, B. Levush, and T. Antonsen, "Tilted Resonator Experiments on a Quasioptical Gyrotron," *Int. J. Electron.* **72**, 807 (1992).

28. R. P. Fischer, A. W. Fliflet, W. M. Manheimer, B. Levush, T. M. Antonsen, Jr., and V. L. Granatstein, "Phase Locking, Amplification, and Mode Selection in an 85 GHz Quasioptical Gyroklystron," *Phys. Rev. Lett.* **72**, 2395 (1994).

29. R. B. McCowan, R. A. Pendleton, and A. W. Fliflet, "Design of an Electron Gun for a 280 GHz Induced-Resonance-Electron-Cyclotron (IREC) Maser Experiment," *IEEE Trans. Elect. Dev.* **39**, 1763 (19992).

30. W. H. Urbanus et al., "A 130-260 GHz, 1 MW Free Electron Laser for Fusion," *Nucl. Instrm. Methods Phys. Res.* **A358**, 155 (1995).

31. J. P. Hogge, T. M. Tran, P. J. Paris, and M. Q. Tran, "Operation of a Quasi-Optical Gyrotron with a Gaussian Output Coupler," submitted to *Phys. Plasmas*, 1996.